

# Synthesis, penetrability and intracellular targeting of fluorescein-tagged peptoids and peptide–peptoid hybrids

Asier Unciti-Broceta, Franziska Diezmann, Chiung Ying Ou-Yang,  
Mario Antonio Fara and Mark Bradley\*

*School of Chemistry, University of Edinburgh, King's Buildings, West Mains Road, Edinburgh EH9 3JJ, UK*

Received 12 November 2007; revised 18 February 2008; accepted 21 February 2008

Available online 26 February 2008

**Abstract**—The search for novel, generally applicable and highly efficient delivery tools is a major activity in the biotechnology arena. Using highly optimized microwave based solid-phase chemistry a series of fluorescein-labelled cationic peptoid conjugates were synthesized within 24 h and cellular uptake into HeLa, L929 and K562 cells examined via flow cytometry. As expected, analysis revealed that longer oligomers achieved greater cellular penetration (**7e** (9 mer) > **7d** (7 mer) > **7c** (5 mer) > **7b** (3 mer) > **7a** (1 mer)) with the nonamer **7e** proving to be a remarkable vehicle for all the cell lines, showing excellent penetrability into K562 and L929 cells and extraordinary cell delivery into HeLa cells. Confocal microscopy showed that the hybrid peptoid–nuclear localizing sequence (PKKKRKV from the simian virus 40 large T antigen) resulted in very high levels of nuclei delivery after 3 h, opening up a range of applications such as nuclei staining of living cells with non-DNA-intercalating fluorescent probes.  
© 2008 Elsevier Ltd. All rights reserved.

## 1. Introduction

To enable entry into cells compounds need to display a bipolar kind of behaviour such that on the one hand they are sufficiently soluble in the media in which the cells are cultured but on the other sufficiently hydrophobic to allow membrane penetration. Such is this dilemma that the solubility properties of any specific compound are often a major factor in determining the efficiency or scope of the molecule being studied often leading to the need to use high doses of material, and high levels of cell mortality. This is a particularly important issue in the fight against the most prevalent of diseases, such as cancer, neurodegeneration and infection, where improving the efficiency of the currently available arsenal of drugs is probably more important than the discovery of new therapeutics or strategies.<sup>1–4</sup>

To solve this delivery issue a number of strategies have been developed to transport poorly permeable materials into cells. For example small sections of the HIV Tat protein (full length 86 amino acids) have been suc-

cessfully used as a ‘Trojan horse’ to enable delivery into cells,<sup>5</sup> with the optimal region of the peptide conferring cell-penetrating properties appearing to be confined to a relatively short stretch of basic amino acids between residues 49 and 57, with the sequence RKKRRQRRR.<sup>6–9</sup> Poly-lysine has similarly been shown to effectively improve the uptake of small organic molecules such as methotrexate,<sup>10</sup> while arginine rich molecules have also been developed to successfully enhance the topical administration of otherwise poorly absorbed drugs such as cyclosporin A<sup>11</sup> and the uptake of sensor molecules.<sup>12</sup> A range of peptidomimetics structurally inspired by the cell-penetrating peptides have been reported by Simon et al.,<sup>13</sup> Wender et al.,<sup>14,15</sup> our group (see Fig. 1),<sup>16</sup> and others,<sup>17</sup> which potentially represent a highly efficient means of translocating a variety of materials across the cell membrane, thus enhancing the pharmacokinetic properties of any drug, sensor or protein.

The work presented here was based on the lysine-like monomeric peptoid, building block **1** and describes: (i) the optimization of the synthesis of the cell-penetrating peptoid derivatives; (ii) studies on the influence of oligomer length on the carrier abilities to enter a variety of cell lines; and (iii) its potential as a general delivery tool for organelle localization, leading to the ability to label cell nuclei.

**Keywords:** Peptidomimetics; Cell-penetrating peptoids; Lysine-like peptoids; Solid-phase synthesis; Peptide–peptoid hybrids; Cellular trafficking; Endocytosis; Nuclear targeting.

\* Corresponding author. Tel.: +44 1316513307; fax: +44 0 1316506453; e-mail: [Mark.Bradley@ed.ac.uk](mailto:Mark.Bradley@ed.ac.uk)

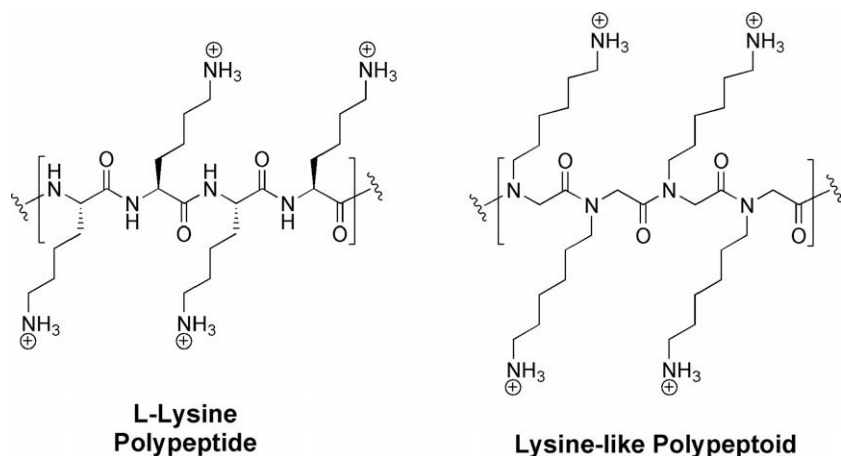


**Figure 1.** Schematic comparison between L-lysine peptides and lysine-like peptoids.

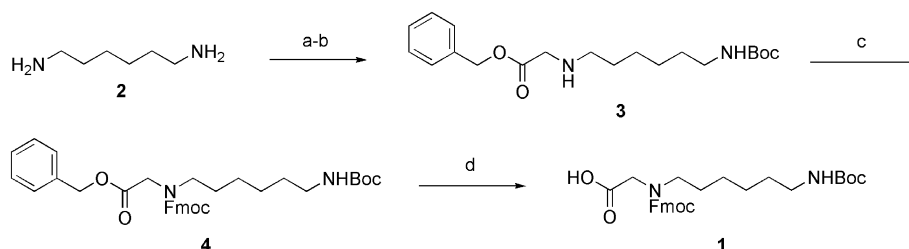
## 2. Results and discussion

### 2.1. Synthesis of peptoids 7a–e

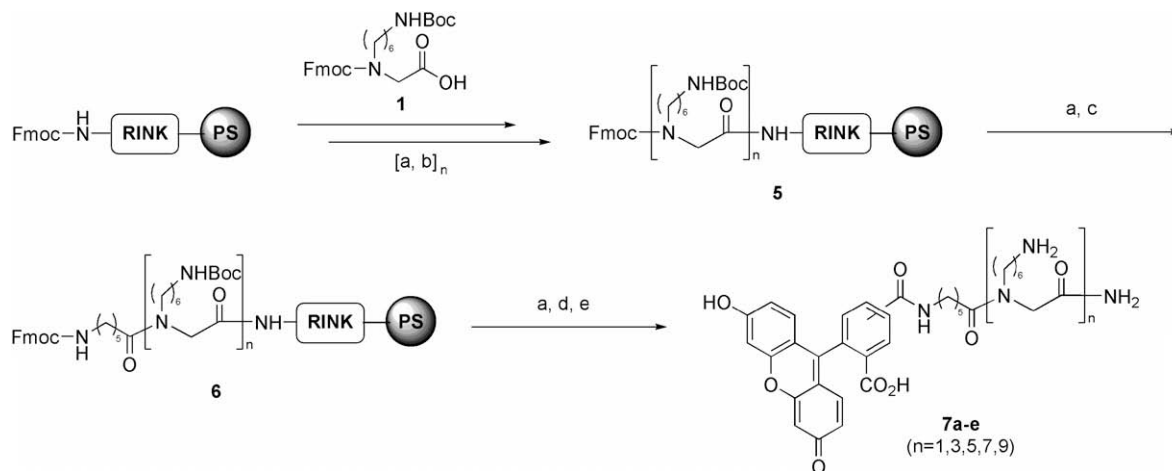
Monomer **1** was prepared from 1,6-hexanediamine **2** following the synthetic pathway shown in **Scheme 1**. Thus diamine **2** was mono-protected using 'Boc anhydride and, without further purification, the remaining primary amine mono-alkylated with benzyl 2-bromacetate in the presence of an excess of triethylamine.<sup>18</sup> The resulting

secondary amine **3** was Fmoc-protected using Fmoc-succinimide before deblocking the benzyl group by catalytic hydrogenation with palladium on charcoal.

The fluorescein-labelled peptoids (**7a–e**) were assembled on aminomethyl polystyrene resin functionalized with a Rink amide linker. This was achieved using a microwave-assisted, Fmoc-based, 'monomer' solid-phase strategy, as illustrated in **Scheme 2**, using lysine-like monomer **1**.<sup>16,18</sup> 5(6)-Carboxy fluorescein was used to



**Scheme 1.** Synthesis of lysine-like monomer **1**. Reagents and conditions: (a)  $\text{Boc}_2\text{O}$  (0.15 equiv), DCM, 14 h; (b) benzyl 2-bromacetate (1 equiv),  $\text{Et}_3\text{N}$  (3 equiv), THF, 24 h, two steps 54%; (c) Fmoc-OSu (1 equiv), THF, 5 h, 90%; (d)  $\text{H}_2$  (1 atm), Pd-C, MeOH, 4 h, 80%.



**Scheme 2.** Synthesis of fluorescein-labelled peptoid oligomers **7a–e** ( $n = 1, 3, 5, 7, 9$ ). Reagents and conditions: (a) 20% piperidine in DMF ( $2 \times 15$  min); (b) monomer **1** (3 equiv), DIC (3 equiv), HOBT (3 equiv), 0.1 M in DMF,  $\mu\omega$ , 60 °C for 20 min; (c) *N*-Fmoc-aminohexanoic acid (3 equiv), reagents and reaction conditions as in (b); (d) 5(6)-carboxy fluorescein (3 equiv), reagents and reaction conditions as in (b); (e) TFA, 2.5% TIS, 2.5%  $\text{H}_2\text{O}$ , 3 h.

label all the peptoids via an aminohexanoic acid spacer.<sup>16</sup> The microwave-assisted procedure significantly reduced coupling times to the secondary amines compared to conventional coupling protocols and dramatically improved yields and overall purities of the process,<sup>19</sup> allowing the preparation of the labelled peptoids, in a single day, with very high purities (>97%).

## 2.2. Screening for cellular uptake

The ability of the fluorescein-tagged peptoids oligomers **7a–e** to enter cells was determined by flow cytometry with human erythroleukaemia (K562), human cervical carcinoma (HeLa) and mouse fibroblast (L929) cell lines. The cells were cultured in their corresponding media and the labelled oligomers (10  $\mu$ M solutions prepared using the extinction coefficient of 5(6)-carboxyfluorescein) were tested in triplicate, using untreated cells and cells incubated with 5(6)-carboxy fluorescein (Fluo) as negative controls, and fluorescein-labelled L-lysine nonapeptide **8** as a positive control. Cells were analyzed at 5 min, 30 min, 2 h and 4 h, using Trypan Blue to quench any extracellular or membrane-associated fluorescence.<sup>20</sup>

As expected<sup>14–16</sup> peptoid uptake was fully dependent on the number of monomer units (see Fig. 2). Higher olig-

omers yielded greater cellular penetration (**7e** (9 mer) > **7d** (7 mer) > **7c** (5 mer) > **7b** (3 mer) > **7a** (1 mer)) as evidenced by a greater population of more intense fluorescently labelled cells. Fluorescence intensity increased in a non-linear manner over time (Fig. 2) pointing to a protein-mediated uptake mechanism, with rapid accumulation within the first 30 min, typically giving half the final uptake observed after 4 h. Generally speaking compound **7e** (9 mer) demonstrated extraordinary cell-penetrating properties, being much better than the shorter oligomers **7a–d** and the positive control L-lysine nonapeptide **8** ((Lys)<sub>9</sub>). As observed in Figure 3, 5(6)-carboxyfluorescein (Fluo) achieved a certain degree of penetrability but lower than compound **7a** (1 mer). The highest alteration of fluorescence intensity was observed in HeLa cells, where compound **7e** (9 mer), in particular, showed quite remarkable cell-penetrating properties with a 70-fold increment of mean fluorescence relative to the untreated cell control after incubating for 4 h. As shown in Figures 2B and 3B a huge leap in activity was observed in going from **7d** (7 mer) and **8** ((Lys)<sub>9</sub>) to **7e** (9 mer) in HeLa cells.

None of the peptoids showed cell toxicity at the concentration tested, as verified by both a propidium iodide as

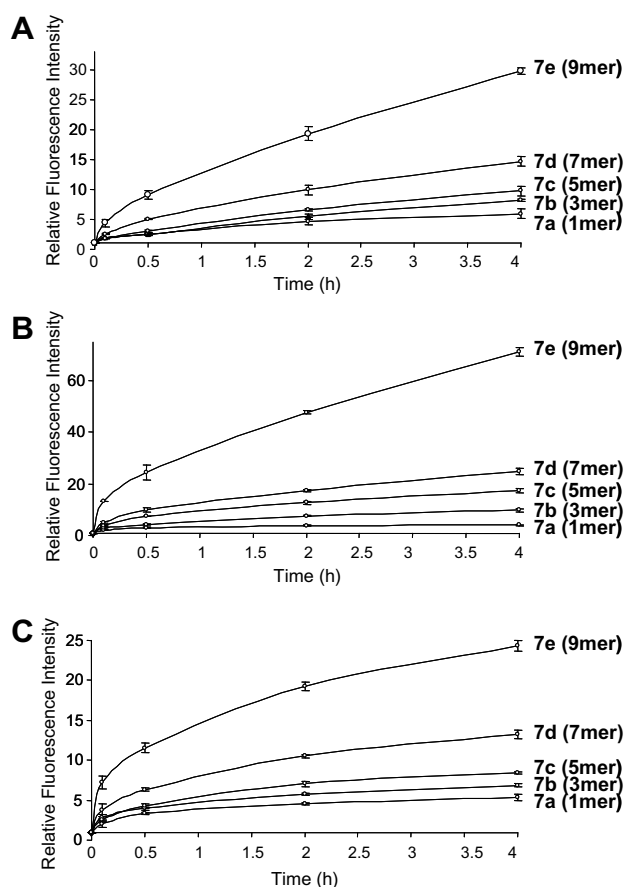


**Figure 2.** Comparative uptake studies of compounds **7a–e** (1–9 mer) as measured via flow cytometry analysis with excitation at 488 nm. Fluorescence intensity is expressed as the mean fluorescence relative to the untreated cell control. Emission was monitored with a 530/30 band-pass filter. (A) K562; (B) HeLa; and (C) L929 cells.

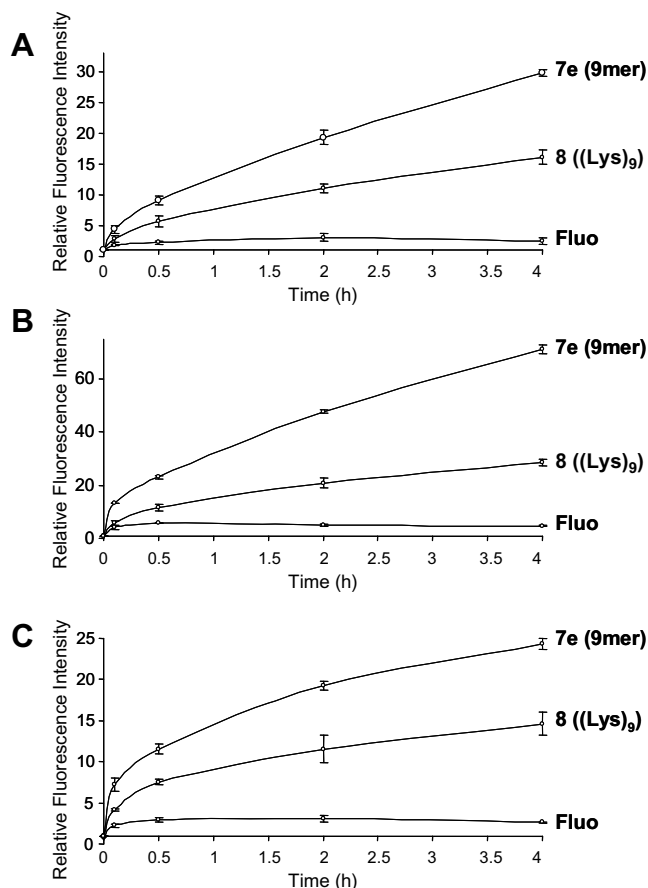


**Figure 3.** Comparative uptake studies of compounds **7e** (9 mer), **8** ((Lys)<sub>9</sub>) and 5(6)-carboxyfluorescein (Fluo) as measured via flow cytometry analysis with excitation at 488 nm. Fluorescence intensity is expressed as the mean fluorescence relative to the untreated cell control. Emission was monitored with a 530/30 band-pass filter. (A) K562; (B) HeLa; and (C) L929 cells.

say (simultaneously carried out during the flow cytometry analysis) and a MTT<sup>21</sup> toxicity assay.

In order to verify the intracellular location of the fluorescein-labelled peptoids, cells incubated with compound **7e** were fixed with paraformaldehyde and analyzed by confocal microscopy (Fig. 4), showing internalization of the peptoids. In Figure 4, two cells were imaged in the anaphase of the mitotic process, clear evidence that the normal behavior of the cells had not been altered by the presence of **7e**.

With the idea of showing if peptoid internalization occurred by endocytosis the fluorescence of ‘live’ cells was examined by confocal microscopy during the first few minutes of incubation with the fluorescein-tagged peptoid **7e**. Before the analysis, cells were washed with a solution of Trypan Blue to reduce the extracellular background.<sup>22</sup> Confocal microscopy (Fig. 5) showed that intracellular fluorescence came from highly local-

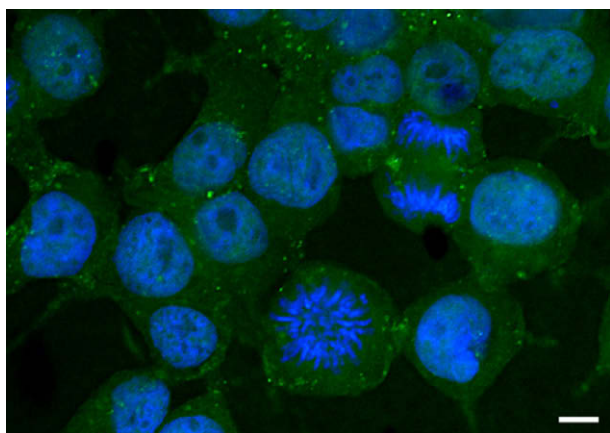


**Figure 4.** Confocal-microscope image of HeLa cells after incubation with compound **7e** (10  $\mu$ M in media) for 2 h. Subsequently cells were fixed, stained with Hoechst 33342 and fluorescently imaged at 407 nm and 488 nm (excitation). Bar = 10  $\mu$ m.

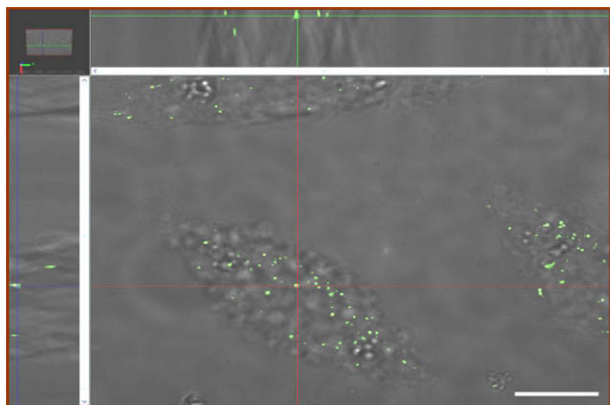


**Figure 5.** Confocal-microscope brightest-point image of live L929 cells after incubating with **7e** (9 mer, 10  $\mu$ M dilution in media) for 10 min. Composite image of brightfield and excitation at 488 nm. Bar = 10  $\mu$ m.

ized ‘fluorescent dots’, which after 30 min became liberated within the cell. Microscopy studies along with the demonstration<sup>16</sup> that the uptake of the lysine-like peptoids was an energy-dependent process supports endocytosis as the main uptake mechanism.

### 2.3. Peptoid–peptide conjugates—nuclei targeting

With the aim of mediating intracellular trafficking 5 mer and 9 mer peptoids were conjugated to the nuclear localizing sequence (NLS) from the simian virus 40 large T antigen (PKKKRKV). This peptide sequence belongs to the group of short amino acid stretches which act as a tag on the exposed surface of some proteins promoting their transport into the cell nucleus, via its recognition by importins,<sup>23</sup> through the nuclear pore complex. It has been reported that the use of this kind of sequence conjugated with a cargo is an efficient and very specific mechanism for transporting different classes of biomaterials, such as nucleotides,<sup>24</sup> peptidic materials<sup>25</sup> and drugs<sup>26</sup> into the nucleus.

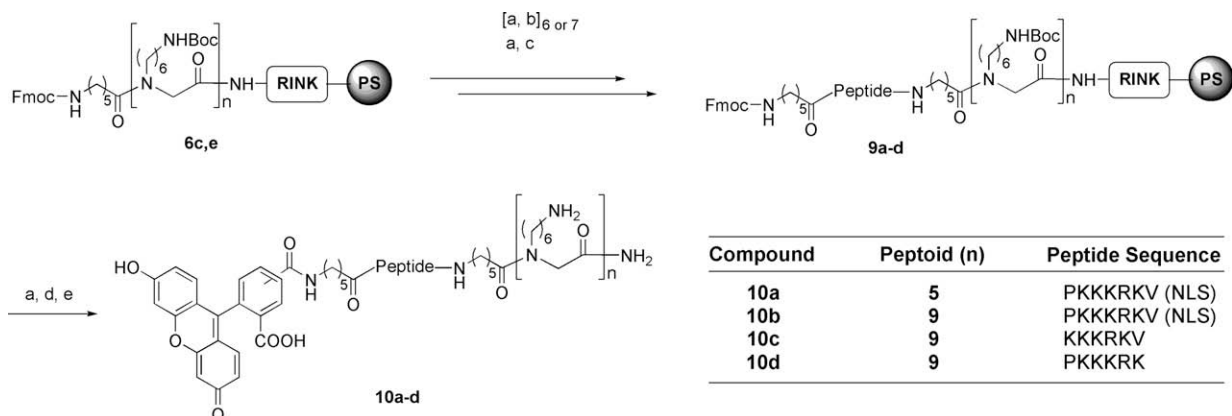
The NLS heptapeptide was therefore assembled onto peptoid resins **6c** and **6e**, following the same microwave-assisted Fmoc-based solid-phase strategy, and then conjugated to the aminohexanoic acid spacer and 5(6)-carboxyfluorescein (see Scheme 3). The overall sequence consisted of a total of 31 and 35 synthetic steps, respectively (coupling, deprotection and cleavage), and gave conjugate **10a** and **10b** in good yields (>92% purity).

The ability of the fluorescein-tagged hybrids **10a** (5 mer-NLS) and **10b** (9 mer-NLS) to enter cells was then tested with HeLa cells and analyzed by flow cytometry. The experiments were carried out in triplicate using untreated cells as a negative control and cells incubated with peptoids **7c** (5 mer) and **7e** (9 mer) as positive controls. As shown in Figure 6, both hybrids showed extraordinary cell-penetrating properties. Compound **10b** (9 mer-NLS) in particular was able to reach, after incubating for 4 h, a 100-fold increase in mean fluorescence relative to the untreated cellular control. It was clear that there was a cooperative effect between peptoid and peptide, resulting in an improvement of cellular uptake of conjugates **10a,b** compared to peptoids **7c,e**. This phenomenon, which more significantly affected the cell-penetrating properties of 5 mer-NLS hybrid **10a**, is consistent with the basic nature of the NLS sequence.<sup>5–10</sup>

Subsequently, the capacity of hybrids **10a,b** to target the cell nuclei was tested with two adherent cell lines: HeLa and human bronchial epithelial cells (16HBE14o-). Compounds **10a,b** were added to cells and incubated for 1 h. Cells were washed with PBS and incubated for 2 h. Subsequently, the cells were fixed and the nuclei stained with Hoechst-33342 prior to analysis by confocal microscopy. As shown in Figure 7, it was clear to observe the co-localization of the hybrid fluorescence emanating from the nucleus along with Hoechst-33342.

Finally, using the same synthetic methodology two analogues of NLS-peptoid hybrid **10b** were prepared in





**Scheme 3.** Synthesis of fluorescein-labelled peptide-peptoid hybrids **10a–d**. Reagents and conditions: (a) 20% piperidine in DMF ( $2 \times 15$  min); (b) Fmoc-protected amino acid (3 equiv), DIC (3 equiv), HOBT (3 equiv), 0.1 M in DMF,  $\mu\omega$ , 60 °C for 20 min; (c) *N*-Fmoc-aminohexanoic acid (3 equiv), reagents and reaction conditions as in (b); (d) 5(6)-carboxy fluorescein (3 equiv), reagents and reaction conditions as in (b); (e) TFA, 2.5% TIS, 2.5% H<sub>2</sub>O, 3 h.

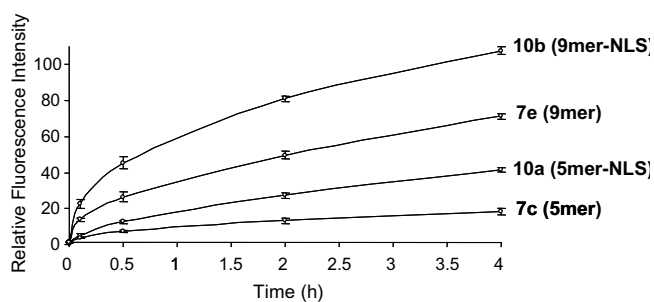


**Figure 6.** Comparative uptake studies of NLS-peptoid hybrids **10a** and **10b** compared to standard peptides **7c** and **7e** in HeLa cells as measured via flow cytometry analysis. Fluorescence intensity expressed as the mean fluorescence relative to the untreated cell control. Excitation at 488 nm, with emission monitored with a 530/30 band-pass filter.

which either the terminal proline or the initial valine residue was omitted to give conjugates **10c** and **d**, respectively (see [Scheme 1](#)). Confocal analysis of their cellular uptake into HeLa cells showed that deletion of these residues resulted in no apparent nuclear targeting after 7 h, verifying the importance of both amino acids for the peptide-protein recognition process, either by enhancing the interaction between the basic amino acids from the NLS and the importin's binding site or by interacting with the importin's signalling domain.<sup>27</sup>

### 3. Conclusions

In conclusion, the efficient chemistry developed for the synthesis of the conjugates permitted the rapid construc-

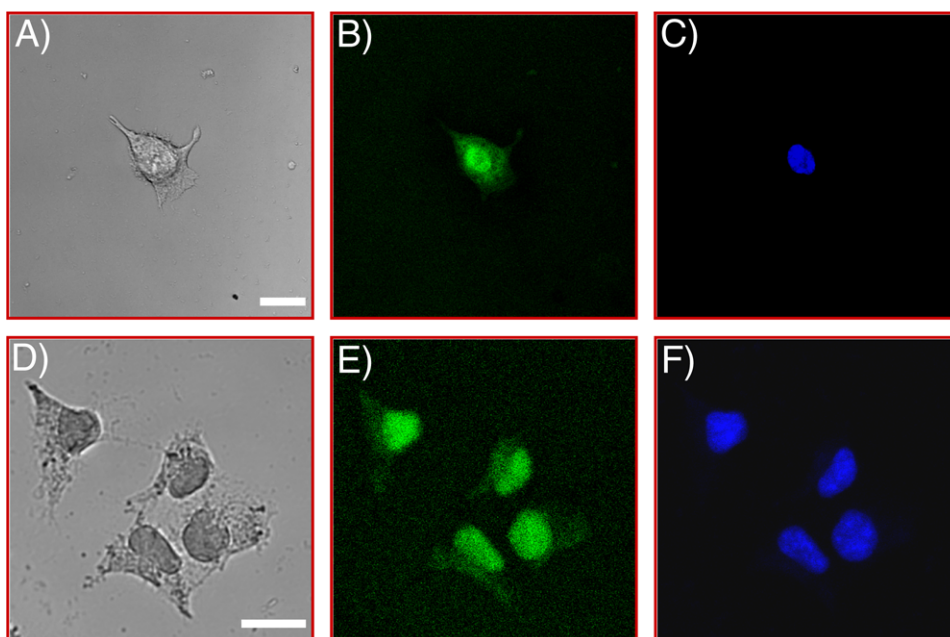


**Figure 7.** Confocal-microscope central-slice images of cells after incubation with hybrid **10b**. (A–C) 16HBE14o-cells. (D–F) HeLa cells. (A and D) Bright-field images. (B and E) Excitation at 488 nm. (C and F) Excitation at 407 nm. Bar = 25  $\mu$ m.

tion of the various tagged peptoids in very high yields and purities. Flow cytometry analysis showed that the ability to enter cells was fully dependent on the number of monomer units. Compound **7e** ( $n = 9$ ) proved to be a quite remarkable carrier for all the cell lines, showing good penetrability into K562 and L929 cells and extraordinary cell delivery properties with HeLa cells, with high entry within 5 min. Additionally, confocal images supported endocytosis as the main uptake mechanism. The NLS-peptoid hybrids allowed specific intracellular trafficking of the fluorescein tag into the nucleus, thus opening up a potential range of applications for specific nuclei delivery of these peptide-peptoid hybrids such as nuclei staining of living cells with non-DNA-intercalating fluorescent probes. Moreover, the absence of nuclear targeting capacity evidenced by hybrids **10c,d** clearly delineates the importance of the role of the proline and valine residues in the peptide-protein interaction between the NLS and the nuclear transporters.

#### 4. Experimental

All chemicals, solvents and biological materials were purchased from Sigma–Aldrich or Fischer.

##### 4.1. Synthesis of lysine-like peptoid unit 1

**4.1.1. Synthesis of benzyl-(6-*tert*-butoxycarbonylamino-hexylamino)-acetate (3).** Di-*tert*-butyl carbonate (5.19 g, 0.0298 mol) in DCM (50 ml) was added dropwise to 1,6-diaminohexane (22.1 g, 0.19 mol) in DCM (100 ml) and the reaction was stirred overnight. The solvent was evaporated and the residue was suspended in H<sub>2</sub>O (100 ml). The insoluble white solid was removed by filtration and the product was then extracted using DCM (3 × 100 ml). The combined organic phase was washed with brine (2 × 50 ml), dried over Mg<sub>2</sub>SO<sub>4</sub> and concentrated in vacuo to give a pale yellow oil. The compound was used for the next step without any further purification. A solution of benzyl 2-bromacetate (5.8 g, 0.025 mol) in THF (20 ml) was added dropwise to a stirred solution of *N*-Boc-1,6-hexanediamine (5.5 g, 0.025 mol) and triethylamine (5.4 g, 0.075 mol) in THF (50 ml) over 2 h, then the reaction was stirred for another 24 h. After filtration of the white solid, the solution was concentrated in vacuo and the crude product was purified by column chromatography using ethyl acetate as eluent to obtain compound **3** as a pale yellow oil (5.0 g, 54%, two steps).

<sup>1</sup>H NMR (300 MHz, CDCl<sub>3</sub>)  $\delta$  1.23–1.31 (m, 4H), 1.36–1.50 (m, 13H), 2.56 (t,  $J = 7.5$  Hz, 2H), 3.03–3.10 (m, 2H), 3.42 (s, 2H), 5.14 (s, 2H), 7.31–7.43 (m, 5H). <sup>13</sup>C NMR (75.5 MHz, CDCl<sub>3</sub>)  $\delta$  26.7, 26.9, 28.5, 30.0, 40.5, 49.5, 51.0, 66.5, 79.0, 128.4, 128.6, 135.7, 156.0, 172.5. HRMS (FAB): C<sub>20</sub>H<sub>32</sub>N<sub>2</sub>O<sub>4</sub>; [M+H]<sup>+</sup>: calc: 365.2440; found: 365.2439.

**4.1.2. Synthesis of benzyl-[(6-*tert*-butoxycarbonylamino-hexyl)-(9H-fluoren-9-ylmethoxycarbonyl)-amino]-acetate (4).** Fmoc-Osu (4.6 g, 0.0137 mol) was added to a solu-

tion of **3** (5.0 g, 0.0137 mol) in DCM (50 ml). The reaction was monitored by TLC until completion (4 h). The solvent was removed in vacuo and the crude product was purified by column chromatography on silica gel (eluent: EtOAc/Hexane, 1:1) to give **4** as a light yellow oil (7.2 g, 90%).

<sup>1</sup>H NMR (300 MHz, CDCl<sub>3</sub>) two rotamers  $\delta$  1.13–1.47 (m, 17H), 3.13 and 3.49 (m, 4H), 3.96 and 4.03 (s, 2H), 4.13 and 4.26 (t,  $J = 6.0$  Hz, 1H), 4.40 and 4.53 (d,  $J = 6.0$  Hz, 2H), 5.13 and 5.18 (s, 2H), 7.27–7.44 (m, 9H), 7.53–7.61 (m, 2H), 7.61–7.79 (m, 2H). <sup>13</sup>C NMR (75.5 MHz, CDCl<sub>3</sub>) two rotamers  $\delta$  26.3, 26.5 and 26.6, 27.9, 28.3 and 28.5, 30.0 and 30.1, 40.5, 47.4, 48.5, 48.8 and 48.9, 49.3, 67.0, 67.4 and 67.6, 79.1, 120.0, 124.9, 125.0, 127.1, 127.7, 128.4, 128.7, 135.4, 135.5, 141.4 and 141.5, 144.1, 155.9 and 156.0, 156.5, 169.6 and 169.7. HRMS (FAB): C<sub>35</sub>H<sub>42</sub>N<sub>2</sub>O<sub>6</sub>; [M+H]<sup>+</sup>: calc 587.3121; found: 587.3113.

**4.1.3. Synthesis of [(6-*tert*-butoxycarbonylamino-hexyl)-(9H-fluoren-9-ylmethoxycarbonyl)-amino]-acetic acid (1).** 10% Pd/C (0.24 g) was added to a solution of **4** (4.0 g, 6.8 mmol) in MeOH (100 ml). The reaction was stirred under hydrogen atmosphere (1 atm) for 4 h at room temperature. The reaction mixture was filtered over Celite and the filtrate concentrated in vacuo. The product was purified by flash chromatography on silica gel (eluent: DCM/MeOH, 10:1) to give **1** as a white solid (2.71 g, 80%).

<sup>1</sup>H NMR (CDCl<sub>3</sub>, 300 MHz) two rotamers  $\delta$  1.3–1.6 (m, 17H); 3.0 and 3.2 (two br m, 4H); 3.30 and 3.4 (br s, 2H); 4.10 (m, 1H); 4.45 and 4.51 (two m, 2H); 7.26 (m, 2H) 7.35 (t,  $J = 7.5$  MHz, 2H); 7.53 (d,  $J = 7.5$  MHz, 2H); 7.72 (d,  $J = 7.0$  MHz, 2H). <sup>13</sup>C NMR (CDCl<sub>3</sub>, 75.5 MHz)  $\delta$  26.4, 27.6, 28.0, 28.5, 29.9, 40.5, 47.1, 48.5, 51.0, 67.5, 78.9, 119.8, 124.8, 126.9, 127.5, 141.2, 143.9, 156.0, 157.5. HRMS (ES<sup>+</sup>): C<sub>28</sub>H<sub>36</sub>N<sub>2</sub>O<sub>6</sub>; [M+Na]<sup>+</sup>: calc 519.2466; found: 519.2456.

##### 4.2. Synthesis of labelled peptoids 7a–c, peptide 8 and peptide-peptoid conjugates 9a–b and 10a–d

The peptoids were assembled on aminomethyl polystyrene resin functionalized with a Rink amide linker using monomer **1**.<sup>19</sup> **Coupling procedure:** Three equivalents of monomer **1**, DIC and HOBt in DMF at a concentration of 0.1 M were mixed with the corresponding resin and microwave irradiated at 60 °C for 20 min. Deprotection of the Fmoc group (20% piperidine in DMF) and repeated coupling (as above) gave the desired oligomers of the required length. These were then coupled to an Fmoc-protected six carbon spacer (Fmoc-aminohexanoic acid) using the coupling procedure described above, deprotected with 20% piperidine in DMF, and conjugated with 5(6)-carboxyfluorescein. Finally, the resin bound peptoids were deprotected and cleaved from the solid support by treatment with a mixture of TFA/TIS/H<sub>2</sub>O (95:2.5:2.5) for 3 h, and precipitated with diethyl ether as pale yellow solids. The crude materials were analyzed by MS (ES<sup>+</sup>) and RP-HPLC (purity assessed via Evaporative Light Scattering detection): **7a**,

calcd for  $C_{35}H_{40}N_4O_8$  645.3, mass found  $m/z$ : 646.3 ( $[M+1]^+$ ), 323.4 ( $[M+2]^{2+}$ ), HPLC purity >98%; **7b**, calcd for  $C_{51}H_{72}N_8O_{10}$  957.2, mass found  $m/z$ : 958.2 ( $[M+1]^+$ ), 479.5 ( $[M+2]^{2+}$ ), 320.1 ( $[M+3]^{3+}$ ), purity >97%; **7c**, calcd for  $C_{67}H_{104}N_{12}O_{12}$  1269.6, mass found  $m/z$ : 635.8 ( $[M+2]^{2+}$ ), 424.2 ( $[M+3]^{3+}$ ), 318.5 ( $[M+4]^{4+}$ ), purity >98%; **7d**, calcd for  $C_{83}H_{136}N_{16}O_{14}$  1582.1, mass found  $m/z$ : 792.0 ( $[M+2]^{2+}$ ), 528.3 ( $[M+3]^{3+}$ ), 396.6 ( $[M+4]^{4+}$ ), purity >97%; **7e**, calcd for  $C_{99}H_{168}N_{20}O_{16}$  1894.5, mass found  $m/z$ : 948.2 ( $[M+2]^{2+}$ ), 632.5 ( $[M+3]^{3+}$ ), 474.7 ( $[M+4]^{4+}$ ), 380.0 ( $[M+5]^{5+}$ ), purity >97%.

L-Lysine nonapeptide **8** was synthesized using *N*-Fmoc-Lys(Boc)-OH following the same procedure as above. The crude material was analyzed by MALDI-TOF MS and RP-HPLC (purity assessed via Evaporative Light Scattering detection): calcd for  $C_{81}H_{132}N_{20}O_{16}$  1640.9, MALDI-TOF MS analysis of the obtained product showed 1641.7 ( $[M+1]^+$ ) as the main peak, purity  $\geq 90\%$ .

Synthesis of conjugates **10a,b** was achieved by sequentially coupling the suitably protected Fmoc-amino acids: **Val**, **Lys(Boc)**, **Arg(Pbf)**, **Lys(Boc)**, **Lys(Boc)**, **Pro**; onto resins **6c,e** using the same procedure (coupling and deprotection) as above. Fmoc-amino hexanoic acid was then covalently attached to the terminal Proline amino acid, deprotected and coupled to fluorescein as above. Following cleavage from the resins (TFA/TIS/ $H_2O$  (95:2.5:2.5) for 3 h), compounds were precipitated with diethyl ether and characterized: **10a**, calcd for  $C_{113}H_{191}N_{27}O_{20}$  2248.7, MALDI-TOF MS analysis of the obtained product showed 2248.7 ( $[M+1]^+$ ) as the main peak, purity  $\geq 92\%$ ; **10b**, calcd for  $C_{145}H_{255}N_{35}O_{24}$  2870.9, MALDI-TOF MS analysis of the obtained product showed 2871.9 ( $[M+1]^+$ ) as the main peak, purity  $\geq 90\%$ .

Conjugate **10c** and **10d** were prepared by coupling the suitably protected Fmoc-amino acids as above. Characterization of **10c**: calcd for  $C_{140}H_{248}N_{34}O_{23}$  2773.9, mass found (MALDI-TOF MS)  $m/z$ : 2774.7 ( $[M+1]^+$ ), purity (ELS detector) >86%. Characterization of **10d**: calcd for  $C_{140}H_{246}N_{34}O_{23}$  2771.9, mass found (MALDI-TOF MS)  $m/z$ : 2772.6 ( $[M+1]^+$ ), purity (ELS detector) >89%.

#### 4.3. Cell uptake assays

Cells were grown in DMEM, RPMI or MEM supplemented with 4 mM glutamine, 10% FCS and 100 U/ml penicillin/streptomycin until 80% confluence. Cells were then suspended using trypsin/EDTA and counted.  $8 \times 10^4$  cells per well were seeded in 24-well plates and incubated overnight (or the required time period). For the confocal assays  $4 \times 10^5$  cells were seeded onto glass coverslip within a 6-well plate. The day afterwards, compounds were mixed with the corresponding medium to give a final concentration of 10  $\mu M$ . The old media were removed from the wells, cells were washed with warm phosphate buffer saline (PBS), and the peptoid/media mixture was added (350  $\mu l$  or 1.6 ml to each 24- or 6-well plate well, respectively). Each experiment was performed in triplicate. After incubation for the desired

time period at 37 °C and 5%  $CO_2$ , cells were washed twice with PBS and then incubated with 1% w/v propidium iodide in PBS for 20 min. Subsequently, cells were washed again with PBS, detached with trypsin/EDTA, harvested with 2% fetal bovine serum (FBS) in PBS, centrifuged and resuspended with 2% FBS in PBS supplemented with Trypan Blue (0.04%) for analyzing using a BD FACSaria flow cytometer. The cells used for imaging by confocal microscopy were fixed with paraformaldehyde (3.5% w/v in PBS) and the nuclei were stained with Hoechst-33342 (1% w/v in PBS).

#### 4.4. Cell viability assays

Twenty-four hours after the addition of the peptoids, cell death was measured using an MTT cell proliferation assay which was performed as previously described.<sup>21</sup> Absorbance was spectrophotometrically measured at 570 nm. 100% cell viability was observed in all experiments.

#### 4.5. Confocal microscopy analysis

Cellular fluorescence of either fixed or living cells was analyzed by confocal microscopy using a DeltaVision RT Microscope under brightfield and laser excitation at 488 nm and 407 nm. For the 'living' cell experiments, cells were washed twice with warm PBS before analysis before extracellular fluorescence was quenched using PBS supplemented with 2% FBS and 0.04% Trypan Blue.

#### Acknowledgments

We thank MRC (A.U.-B.) for funding. We would like to thank Dr. D.C. Boyd for kindly supplying the 16HBE14o-cells.

#### References and notes

- Lavan, D. A.; Lynn, D. M.; Langer, R. *Nat. Rev. Drug Discov.* **2002**, *1*, 77–84.
- Reis, C. P.; Neufeld, R. J.; Ribeiro, A. J.; Veiga, F. *Nanomedicine* **2006**, *2*, 53–65.
- Reshetnyak, Y. K.; Andreev, O. A.; Lehnert, U.; Engelman, D. M. *Proc. Natl. Acad. Sci. U.S.A.* **2006**, *103*, 6460–6465.
- Roy, I.; Gupta, M. N. *Chem. Biol.* **2006**, *10*, 1161–1171.
- Brooks, H.; Lebleu, B.; Vives, E. *Adv. Drug Del. Rev.* **2005**, *57*, 559–577.
- Ruben, S.; Perkins, A.; Purcell, R.; Joung, K.; Sia, R.; Burghoff, R.; Haseltine, W. A.; Rosen, C. A. *J. Virol.* **1989**, *63*, 1–8.
- Fawell, S.; Seery, J.; Daikh, Y.; Moore, C.; Chen, L. L.; Pepinsky, B.; Barsoum, J. *Proc. Natl. Acad. Sci. U.S.A.* **1994**, *91*, 664–668.
- Vives, E.; Brodin, P.; Lebleu, B. *J. Biol. Chem.* **1997**, *272*, 16010–16017.
- Futaki, S.; Suzuki, T.; Ohashi, W.; Yagami, T.; Tanaka, S.; Ueda, K.; Sugiura, Y. *J. Biol. Chem.* **2001**, *276*, 5836–5840.
- Ryser, H. J. P.; Shen, W.-C. *Proc. Natl. Acad. Sci. U.S.A.* **1978**, *75*, 3867–3870.

11. Rothbard, J. B.; Garlington, S.; Lin, Q.; Kirschberg, T.; Kreider, E.; McGrane, P. L.; Wender, P. A.; Khavari, P. A. *Nat. Med.* **2000**, *6*, 1253–1257.
12. Jones, L. R.; Goun, E. A.; Shinde, R.; Rothbard, J. B.; Contag, C. H.; Wender, P. A. *J. Am. Chem. Soc.* **2006**, *128*, 6526–6527.
13. Simon, R.; Kania, R. S.; Zuckermann, R. N.; Huebner, V. D.; Jewell, D. A.; Banville, S.; Ng, S.; Wang, L.; Rosenberg, S.; Marlowe, C. K.; Spellmeyer, D. C.; Tan, R.; Frankel, A. D.; Santi, D. V.; Cohen, F. E.; Bartlett, P. A. *Proc. Natl. Acad. Sci. U.S.A.* **1992**, *89*, 9367–9371.
14. Wender, P. A.; Mitchell, D. J.; Pattabiraman, K.; Pelkey, E. T.; Steinman, L.; Rothbard, J. B. *Proc. Natl. Acad. Sci. U.S.A.* **2000**, *97*, 13003–13008.
15. Wender, P. A.; Rothbard, J. B.; Jessop, T. C.; Kreider, E. L.; Wylie, B. L. *J. Am. Chem. Soc.* **2002**, *124*, 13382–13383.
16. Peretto, I.; Sanchez-Martin, R. M.; Wang, X. H.; Ellard, J.; Mitto, S.; Bradley, M. *Chem. Commun.* **2003**, 2312–2313.
17. Umezawa, N.; Gelman, M. A.; Haigis, M. C.; Raines, R. T.; Gellman, S. H. *J. Am. Chem. Soc.* **2002**, *124*, 368–369.
18. Kruijtz, J. A. W.; Liskamp, R. M. J. *Tetrahedron Lett.* **1995**, *36*, 6969–6972.
19. Fara, M. A.; Díaz-Mochón, J. J.; Bradley, M. *Tetrahedron Lett.* **2006**, *47*, 1011–1014.
20. Hed, J.; Hallden, G.; Johanson, G.; Larsson, P. *J. Immunol. Methods* **1997**, *101*, 119–125.
21. Mossman, T. *J. Immunol. Methods* **1983**, *65*, 55–63.
22. Rejman, J.; Oberle, V.; Zuhorn, I. S.; Hoekstra, D. *Biochem. J.* **2004**, *377*, 159–169.
23. Jans, D. A.; Xiao, C.-Y.; Lam, M. H. C. *BioEssays* **2000**, *22*, 532–544.
24. Zanta, M. A.; Belguise-Valladier, P.; Behr, J.-P. *Proc. Natl. Acad. Sci. U.S.A.* **1999**, *96*, 91–96.
25. Chen, P.; Wang, J.; Hope, K.; Jin, L.; Dick, J.; Cameron, R.; Brandwein, J.; Minden, M.; Reilly, R. M. *J. Nucl. Med.* **2006**, *47*, 827–836.
26. Sibrian-Vazquez, M.; Jensen, T. J.; Hammer, R. P.; Vicente, M. G. H. *J. Med. Chem.* **2006**, *49*, 1364–1372.
27. Nguyen, J. T.; Turck, C. W.; Cohen, F. E.; Zuckermann, R. N.; Lim, W. A. *Science* **1998**, *282*, 2088–2092.